

## Detailed optical studies of several banana-shaped compounds in liquid crystal B2 phase

D. A. Olson,<sup>1</sup> A. Cady,<sup>1</sup> W. Weissflog,<sup>2</sup> H. T. Nguyen,<sup>3</sup> and C. C. Huang<sup>1</sup><sup>1</sup>*School of Physics and Astronomy, University of Minnesota, Minneapolis, Minnesota 55455*<sup>2</sup>*Institute für Physikalische Chemie, Martin-Luther-Universität Halle-Wittenberg, Mühlpforte 1, D-06108 Halle, Germany*<sup>3</sup>*Centre de Recherche Paul Pascal, CNRS, Université Bordeaux I, Avenue A. Schweitzer, F-33600 Pessac, France*

(Received 27 April 2001; published 26 October 2001)

Null-transmission ellipsometry has been performed on free-standing films of one compound in the liquid crystal B2 phase. We have studied films of thickness from 1 to 121 layers. One of the compounds used has an unusually wide 59 K window for the B2 phase. The tilt angle was investigated as a function of temperature and found to be constant over this temperature range to within our resolution of 1°. The one-layer films studied exhibit the same structure as the thicker films, and have helped us to refine the optical model for the B2 phase. For thin films we find that modeling a single smectic layer as two uniaxial layers is a better description of the data than a single biaxial layer, but that for thick films the model used does not effect the simulated result appreciably. Preliminary results also find that the surface layers are less tilted than the interior layers, in contrast to rodlike liquid crystals, which show an enhanced surface tilt.

DOI: 10.1103/PhysRevE.64.051713

PACS number(s): 61.30.Gd, 83.80.Xz

## I. INTRODUCTION

The discovery of ferroelectric [1] and antiferroelectric [2] ordering in chiral, rod-shaped liquid crystals created a lot of excitement in condensed-matter physics. However, it was generally assumed that chirality in the molecule was necessary to break the mirror symmetry and create ferroelectric or antiferroelectric ordering. In 1994, Watanabe *et al.* [3] proposed that antiferroelectric and ferroelectric ordering may appear in systems of achiral molecules if the molecules are packed with  $C_{2v}$  symmetry. This packing is possible with banana-shaped molecules because of their shape, as was discovered in 1996 by Niori *et al.* [4] One of the phases formed by banana-shaped molecules that has attracted interest is the B2 phase because of its antiferroelectric properties.

Link *et al.* [5] proposed models for the B2 phase based upon electro-optical studies of free-standing films and bulk cells. In bulk cells they found four different layer arrangements. The predominant state at zero field is shown in Fig. 1(a). In free-standing films only one layer structure was seen [see Fig. 1(b)]. We have been able to confirm their results for free-standing films [6]. The B2 phase can be described as follows. The molecules are arranged into layers, with no long-range positional ordering within each layer. The long axes of the molecules are tilted at an angle  $\theta$  to the layer normal. Within each layer the molecules are aligned, so a vector  $\mathbf{b}$  can be defined that points along the bend of the molecule [see Fig. 1(c)]. In free-standing films the orientation of the tilt is parallel in adjacent layers, but  $\mathbf{b}$  is antiparallel. The polarization points either parallel or antiparallel to  $\mathbf{b}$ , depending on the compound. Films with an even  $N$  have no net polarization, while films with an odd  $N$  have a net polarization associated with the one layer whose polarization is not cancelled. Thus it is possible to align films of an odd  $N$  with a small electric field.

In the B2 phase, the layer spacing ( $d$ ) has been found experimentally to decrease with increasing temperature [7] for several compounds. This suggests that the molecular tilt angle ( $\theta$ ) relative to the layer normal increases with increas-

ing temperature, which is inconsistent with recent theoretical advances [8] that propose  $\theta$  is a principal order parameter.

Ordinarily  $\theta$  can be determined by measurements on a well-aligned bulk sample between two pieces of glass.  $\theta$  is obtained by measuring the orientation of the optic axis under a large applied electric field [9] or from x-ray diffraction by measuring the angle that the chevrons make with respect to the normal of the glass surface [10]. However, to the authors' knowledge, no one has yet been able to produce well-aligned bulk samples. Of late we have developed a technique to measure  $\theta$  for compounds in the B2 phase using null-transmission ellipsometry (NTE) in the free-standing film geometry [6]. With this unique system we decided that it was necessary to measure the temperature dependence of  $\theta$  for two reasons. First, to our knowledge, dependence of  $\theta$  on temperature has not been reported before for any compound in the B2 phase. Second, we wished to resolve the issue discussed above.

We applied our technique to a recently synthesized compound, (14PMB)Cl [see Fig. 2(a)], exhibiting a 59 K wide B2 temperature window [11]. The phase sequence for this compound is crystal  $\rightarrow$  (68 °C)  $\rightarrow$  B2  $\rightarrow$  (127 °C)  $\rightarrow$  isotropic.  $d$  was measured by x-ray diffraction on a powder sample

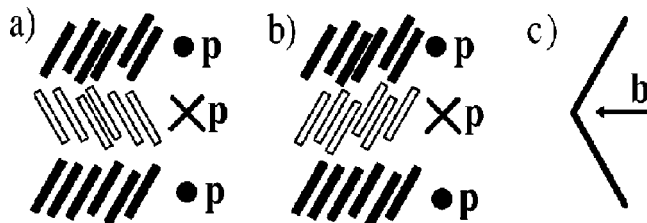


FIG. 1. (a) The predominant layer structure of the B2 phase found in bulk samples. The molecules drawn solid have  $\mathbf{b}$  pointing out of the page, while the molecules drawn hollow have  $\mathbf{b}$  pointing into the page. Although the polarization  $\mathbf{p}$  is shown parallel to  $\mathbf{b}$ , it can also be antiparallel depending on the compound. (b) The layer structure of the B2 phase seen in free-standing films. (c) The vector  $\mathbf{b}$  is shown pointing along the bend of the molecule.

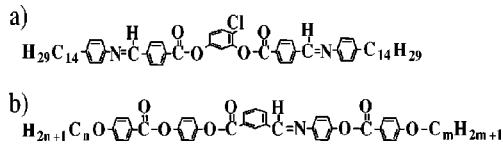


FIG. 2. (a) and (b) show the molecular structure for (14PMB)Cl and  $C_{n,m}$ , respectively. The bend in the molecule is provided by the bonds to the central benzene ring. The molecule is drawn straight to save space.

using a rotating-anode machine. Our NTE setup was used to measure the temperature dependence of  $\theta$  in the B2 phase. Forty-one free-standing films of thickness ranging from  $N = 1$  to 121 layers were studied, where  $N$  is the number of layers in the film. We found that  $\theta$  is independent of temperature to within our resolution of  $1^\circ$ . The results from one-layer films have allowed us to refine the optical model of the B2 phase. We have also reanalyzed our data from the  $C_{8,12}$  and  $C_{9,12}$  compounds [see Fig. 2(b)] previously studied [6] using this refined model. The simulated  $\theta$  is found to be the same for both modeling techniques. We have also found evidence for an unusual reduced tilt at the surface layers of the film, which is independent of the optical model used.

## II. METHOD

Free-standing films were used because films, unlike bulk cells, provide excellent uniform alignment of the layers. All the films, except for the one-layer films, were drawn across a 7-mm-diam hole in a glass cover slip. The one-layer films were drawn across a smaller 3-mm-diam hole because of the difficulty in spreading a one-layer film over a large area. Eight electrodes surrounding these holes allowed for the application of an electric field of 1 to 10 V/cm. These fields are large enough to orient the films without inducing flow or distorting the zero-field structure. The electrodes allowed us to rotate the direction of the electric field smoothly within the plane of the sample. By observing the orientation of the c-director using depolarized reflected light microscopy and by numerical calculations we have found that the orientation of the electric field is very uniform in the plane of the film except near the electrodes. The films were created in a temperature-regulated sealed oven with argon as an exchange gas.

Our NTE [12] setup was used to acquire the optical properties of the samples. We have shown that our NTE approach can be used to measure  $\theta$  accurately [13]. The ellipsometric parameters  $\Delta$  and  $\Psi$  are measured with a resolution of  $0.001^\circ$  using the polarizer-compensator-sample-analyzer configuration.  $\Delta$  is the phase lag between the  $p$  and  $s$  components of the light incident upon the sample necessary to produce linearly polarized transmitted light.  $\Psi$  is the angle of the polarization of the transmitted light.  $\Delta$  and  $\Psi$  depend upon the optical structure and orientation of the sample. The incident angle of the laser beam is  $45^\circ$  to the layer normal of the film.

Experimentally, we found that it is much easier to create free-standing films by heating the sample to  $130^\circ\text{C}$  (the isotropic phase) and then cooling to  $125^\circ\text{C}$  (the B2 phase). This

process wets the spreader with compound. Wetting does not occur rapidly in the B2 phase.

Once the film was created, it was cooled to  $120^\circ\text{C}$  and allowed to become uniform in thickness. If the film was one-layer thick we cooled to  $110^\circ\text{C}$  instead of  $120^\circ\text{C}$  because these films were unstable at  $120^\circ\text{C}$ . Then we began to take ellipsometric data while rotating the electric field with a step size of  $12^\circ$ . After several rotations we would cool by steps of 10 K and begin rotations at the new temperature. This procedure was repeated until a temperature of  $70^\circ\text{C}$  was reached.

By this method  $\Delta$  and  $\Psi$  were acquired for complete rotations, providing the film had a net polarization, for a series of temperatures. Several rotations were conducted at each temperature to check for reproducibility. If the film did not align due to the electric field, i.e., it had an even  $N$ , then data were taken while the film reoriented due to thermal fluctuations. We lose orientational information by this approach, but can still plot  $\Psi$  vs  $\Delta$  to get a characteristic shape that depends on the optical structure of the film. Such films need not yield data points for a complete rotation. Because of this difficulty, only films that responded to the electric field were studied as a function of temperature. However, we needed the data from one temperature for some films with an even  $N$  to determine  $N$  in the films studied, as is described below.

## III. RESULTS AND ANALYSES

In this section our results are presented and analyzed. We begin by looking at the data qualitatively in order to find what can be learned at a simple level. Our method of simulating the data is then presented, along with our technique at finding the necessary optical parameters. The data demonstrating our need for a different optical model than previously used are then discussed. The results of the simulations of thick films are then presented, and our findings for the temperature dependence of the optical parameters. A reanalysis of our results for  $C_{8,12}$  and  $C_{9,12}$  follows. Finally, evidence is given for a reduced tilt on the surface layers of the film.

Figure 3 shows  $\Psi$  and  $\Delta$  vs  $\alpha$  from rotations of a  $47 \pm 2$  layer film at  $120^\circ\text{C}$  (squares),  $100^\circ\text{C}$  (circles), and  $70^\circ\text{C}$  (stars).  $\alpha$  (shown in the inset) is the angle between the applied electric field ( $\mathbf{E}$ ) and the incidence plane of the laser beam. The method to determine the thickness is described below.

$\Delta$  should have its maximum variance from  $\Delta$  averaged over one rotation ( $\Delta_{\text{AVG}}$ ), shown as a dashed line for the data at  $120^\circ\text{C}$  for Fig. 3, where the optical path difference between the  $p$  and  $s$  components of the light is greatest. Because the long axis of the molecules are aligned throughout the film in the B2 phase, the above should occur when the long axis of the molecule is as close as possible to perpendicular to the laser beam. This orientation of the long axis implies that the tilt plane is in the incidence plane of the laser. If one ignores multiple reflections, then the reason for this orientation to give the maximum variance in  $\Delta$  from  $\Delta_{\text{AVG}}$  can be explained as follows. At this orientation the

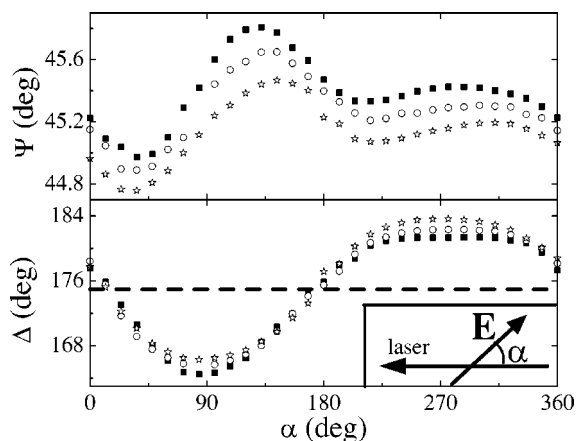


FIG. 3.  $\Psi$  and  $\Delta$  for (14PMB)Cl are shown versus electric-field orientation ( $\alpha$ ) for a  $47 \pm 2$  layer film. The data were taken at  $120^\circ\text{C}$  (squares),  $100^\circ\text{C}$  (circles), and  $70^\circ\text{C}$  (stars).  $\Delta$  averaged over one rotation for  $120^\circ\text{C}$  is shown as a dashed line. The angle  $\alpha$  is shown in the inset as the angle between the incident plane of the laser beam and  $\mathbf{E}$ .

$p$ -component of the polarization probes the maximum amount of the index of refraction along the long axis of the molecule (the largest index of refraction) and the optical path to traverse the film is at a maximum. The  $s$  component is perpendicular to the long axis of the molecule and thus travels the smallest possible optical path. Our data from this and other films implies that the tilt plane of the film aligns at  $90 \pm 5^\circ$  to  $\mathbf{E}$ . Our resolution in this angle is limited both by the noise in our data and the accuracy of the positioning of the electrodes on the glass plate. This observation supports a polarization perpendicular to the tilt plane.

The temperature variation in the average value of  $\Delta$  and  $\Psi$  implies that the optical thickness decreases with increasing temperature. This is consistent with  $d$  decreasing with increasing temperature.

To learn more from our data, the  $4 \times 4$  matrix method [14] was used to simulate  $\Psi$  and  $\Delta$ . In our previous analysis of data in the B2 phase we used a biaxial ellipsoid of refraction to simulate our data [6]. However, our new data from one-layer films is not consistent with this model. Instead each layer of molecules in the B2 phase is simulated as two uniaxial layers of half the thickness. The uniaxial layers are oriented the same as the two legs of the banana-shaped molecules (see Fig. 4). The variables required to describe this model are the bend angle ( $\phi$ ) at the core of the banana-shaped molecules,  $\theta$  the extraordinary ( $n_e$ ) and ordinary ( $n_o$ ) indices of refraction of the uniaxial layers  $d$  and  $N$ .

The tilt angle  $\theta_u$  of the long axis of the legs of the banana-shaped molecules from the layer normal, and thus the tilt angle of the uniaxial ellipsoids of refraction, can be shown to be  $\arccos[\cos(\theta)\cos(\phi)]$ . The relative azimuth between the uniaxial layers is  $(\pi - 2) \arccos[\sin(\phi)/\sin(\theta_u)]$ . The layer spacing of the uniaxial layers is  $d/2$ . The uniaxial layers are then stacked up in pairs so that the long axes of the uniaxial ellipsoids of refraction are aligned parallel to their next-nearest neighbors.

In order to reduce the number of fitting parameters,  $d$  is

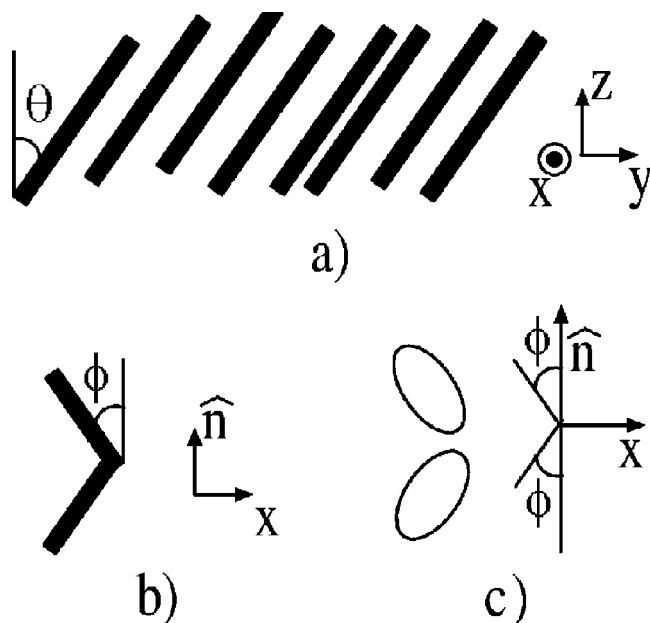


FIG. 4. (a) is a cartoon of a single layer of the B2 phase in the layer reference frame, the molecules are drawn solid to represent  $\mathbf{b}$  pointing out of the page. (b) is a cartoon of a molecule in the molecular reference frame. (c) shows the optical model representing a single layer of molecules in the molecular reference frame. The uniaxial ellipsoids of refraction are oriented along the two legs of the banana-shaped molecule.  $\mathbf{x}$  points along  $\mathbf{b}$ ,  $\mathbf{z}$  points along the layer normal, and  $\mathbf{y}$  is in the tilt plane and perpendicular to  $\mathbf{z}$ .  $\hat{\mathbf{n}}$  points along the long axis of the molecules.  $\theta$  and  $\phi$  are shown.

found by x-ray diffraction. The results for  $d$  are shown in Fig. 5 for (14PMB)Cl.  $d$  decreases linearly as the temperature increases over this temperature range. From comparing the layer spacing to a molecular length of  $61.5 \pm 1.5 \text{ \AA}$ , as was estimated from the molecular structure, it is clear that the layer structure is not a bilayer.

The next step in fitting is to determine the number of layers in each film studied. To determine  $N$  for thin films, a series of films must be pulled. Each film gives a characteristic  $\Psi$  and  $\Delta$  curve upon rotation, which is a function of both the optical thickness and biaxiality in the layer reference frame. When averaged over one rotation,  $\Psi$  and  $\Delta$  depend primarily on the optical thickness and therefore  $N$ . The average  $\Psi$  and  $\Delta$  change in discrete steps due to the quantization of  $N$  and there is a thickness dependant trend. Data from a series of films separated by one layer in thickness is required to be certain that the correct  $N$  is determined for each film. As an independent check,  $N$  was estimated from the color of white light reflected off of the film [15]. Once  $N$  has been found for thin films, the optical parameters can be found by

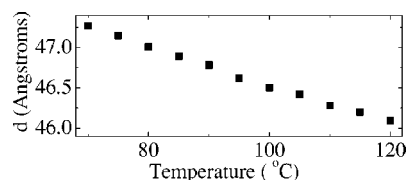


FIG. 5.  $d(T)$  for (14PMB)Cl.

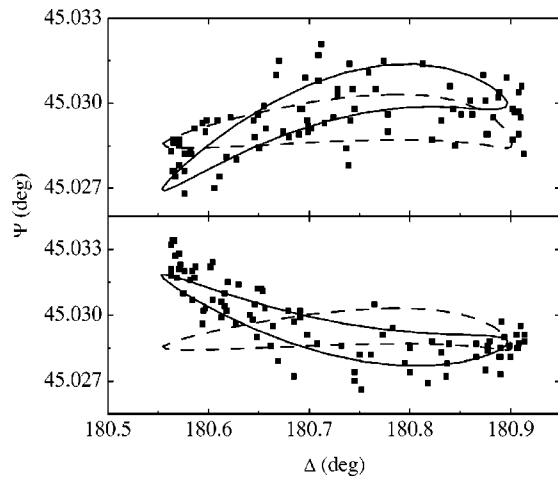


FIG. 6. The top and bottom graphs show data (symbols) and simulations (lines) of the  $\Psi$  versus  $\Delta$  curves for the two handednesses of a one-layer film of (14PMB)Cl. The biaxial fit is shown with a dashed line. The fit obtained from two uniaxial layers (solid lines) uses the parameters  $\theta=30^\circ$  and  $d=49.4 \text{ \AA}$  while the other parameters come from the simulations of thick films.

the method described below. The optical parameters can in turn be used to determine  $N$  for thicker films and then to resolve  $\theta$ .

To determine the remaining optical parameters ( $\theta$ ,  $\phi$ ,  $n_e$ , and  $n_o$ ),  $\Psi$  and  $\Delta$  are simulated as a function of  $\alpha$  for films of odd  $N$  and compared to the measured value. The best fit is found by minimizing the mean-squared deviation of the data from the simulations. It was found that only one set of optical parameters gave the best fit for a fixed  $N$  and  $d$ . This fitting procedure allows us to make a further check on our measurement of  $N$ . If  $N$  has been determined incorrectly then the simulated indices of refraction will be different for different film thicknesses in order to create the correct optical thickness.

Data from thin films, which demonstrates the need for our refined optical model, are shown in Figs. 6 and 7. Figure 6 displays the ellipsometric data (squares) from a one-layer film of both handednesses of (14PMB)Cl at  $80^\circ\text{C}$ . The two handednesses are possible because there are two directions  $\mathbf{b}$  can point, which are perpendicular to the tilt plane of equal

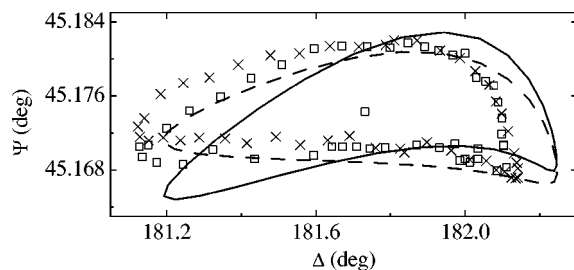


FIG. 7. This graph shows data (symbols) and simulations (lines) of the  $\Psi$  versus  $\Delta$  curves for the two handednesses of a three-layer film of  $\text{C}_{8,12}$ . The simulations are made with the surface layers which are less tilted than the center layer. In the simulations, the optical parameters found from the simulations are used in all cases except that the surface layers use  $\theta=40^\circ$  and  $d=42.2 \text{ \AA}$ .

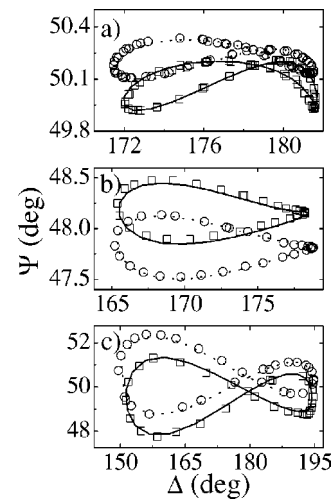


FIG. 8. (a), (b), and (c) show data and simulations of the  $\Psi$  versus  $\Delta$  curves of (14PMB)Cl for  $N=27\pm 2$ ,  $37\pm 2$ , and  $121\pm 4$  layers, respectively. The data taken at  $120^\circ\text{C}$  (squares) and  $70^\circ\text{C}$  (circles) are shown. Simulations of the data are shown with solid and dashed lines for  $120^\circ\text{C}$  and  $70^\circ\text{C}$ , respectively. The details are described in the text.

energy. The data for the two handednesses are shown in separate graphs because of the small signal-to-noise ratio. In Fig. 6, the best fit with the biaxial model is shown with a dashed line, while the best fits for the two uniaxial layer model are shown as a solid lines. Figure 7 displays the ellipsometric data (squares and x's) from a three-layer film of both handednesses of  $\text{C}_{8,12}$  at  $125^\circ\text{C}$ . In this figure the simulations using the best fits to the uniaxial layer model for the two handednesses are shown as lines. The simulations use a reduced surface tilt, as is discussed in more detail below, because this greatly improved the fits. In both figures the two handednesses are from the same film; domains of different handedness moved into the region of the film that the laser beam probes. This process takes a significant amount of time, and we have no way in which to cause the domain to switch. For this reason the data from the one and three-layer films are from different compounds.

From this data, it can be seen that a biaxial ellipsoid of refraction is not a good description of a one-layer film. In the biaxial model, a  $180^\circ$  rotation around any of the major axes leaves the ellipsoid of refraction unchanged. So if  $\mathbf{b}$  rotates by  $180^\circ$  along the long axis of the molecule, which corresponds to a chirality change in the film, then the ellipsoid of refraction remains unchanged although the polarization reverses direction. This predicts that  $\Psi$  versus  $\Delta$  should look identical for both handednesses although  $\Psi$  and  $\Delta$  versus  $\alpha$  should be offset by  $180^\circ$ . What is observed experimentally is that the two handedness give different  $\Psi$  versus  $\Delta$  curves.

For this reason we decided to model the single molecular layer as two uniaxial layers stacked upon each other. This model adds off-diagonal terms to the index of refraction tensor in the molecular reference frame, as well as a reflection at the center of each molecular layer. The model yields good simulations of the data. There is an offset in  $\Delta$  between the simulations and the data, which may be due to the molecule



at the surface having a different conformation than in the interior of the film. The difference between the data and simulations is more than an offset, suggesting that the two uniaxial layers optical model does not perfectly describe the data. The fits use a smaller  $\theta$  than is found in thicker films as is discussed in further detail below. The difference between the data from the two handednesses of a one-layer film is large, but for a three-layer film the difference is subtle. For films of  $N \geq 5$  layers the difference between the predicted  $\Psi$  versus  $\Delta$  curves for the two handednesses becomes negligible.

The data from (14PMB)Cl films of  $N = 27 \pm 2$ ,  $37 \pm 2$ , and  $121 \pm 4$  layers are shown in Fig. 8(a), 8(b), and 8(c), respectively. The data taken at  $120^\circ\text{C}$  (squares) and  $70^\circ\text{C}$  (circles) are shown. The simulations of the data are shown with solid and dashed lines for  $120^\circ\text{C}$  and  $70^\circ\text{C}$ , respectively.

Qualitatively, the following can be learned from the data. The  $\Psi$  and  $\Delta$  curves from different temperatures are approximately the same width, thereby suggesting that  $\theta$  is independent of temperature. The shape is seen to change with temperature, as can be seen most clearly in the Fig. 8(a). This suggests that  $\phi$  or the indices of refraction are changing with temperature.

Only the parameters found from simulating the (14PMB)Cl data for  $N = 27 \pm 2$ ,  $29 \pm 2$ ,  $37 \pm 2$ ,  $47 \pm 2$ , and  $121 \pm 4$  layers are given here because the simulation results from thick films have a higher precision in the optical parameters than thin films. The simulations of these thick films are made assuming that all layers have the same optical parameters. We found that  $\theta$  does not change with temperature within our resolution and equals  $34 \pm 1^\circ$ . The following parameters are reported only at the hottest and coldest temperatures studied because their change due to temperature approaches our resolution on these parameters.  $\phi$  changes from  $24.6 \pm 0.6^\circ$  at  $120^\circ\text{C}$  to  $26.6 \pm 0.6^\circ$  at  $70^\circ\text{C}$ .  $n_o$  changes from  $1.488 \pm 0.009$  at  $120^\circ\text{C}$  to  $1.500 \pm 0.009$  at  $70^\circ\text{C}$ , and  $n_e$  changes from  $1.69 \pm 0.01$  at  $120^\circ\text{C}$  to  $1.71 \pm 0.01$  at  $70^\circ\text{C}$ . The error bars are from the standard deviations of the simulation parameters from these five different films.

$\theta$  has been measured to be  $40^\circ \pm 3^\circ$  for (14PMB)Cl by applying a large electric field to a bulk sample between glass plates [11]. The discrepancy between this result and ours is probably due to the electroclinic effect creating a larger  $\theta$  in a large electric field than is found in zero field. Weissflog *et al.* [11] have directly measured the x-ray tilt angle ( $35^\circ \pm 2^\circ$ ) for a compound in the same homologous series as (14PMB)Cl by using a long annealing process on a glass plate. This technique requires no aligning field and is in agreement with our results.

Our observed temperature variation in  $\phi$  is not unexpected. The chlorine atom was placed at the center of (14PMB)Cl to cause  $\phi$  to change with temperature. This was hoped to induce a phase transition from the B2 phase to phases seen with rod-shaped molecules, such as smectic-A.

In our previous paper [6] we studied  $C_{8,12}$  and  $C_{9,12}$ . The data were simulated with a biaxial ellipsoid of refraction. We have reanalyzed the data using the optical model presented herein and found that the tilt angle remained the same as that found using a biaxial ellipsoid of refraction. We have per-

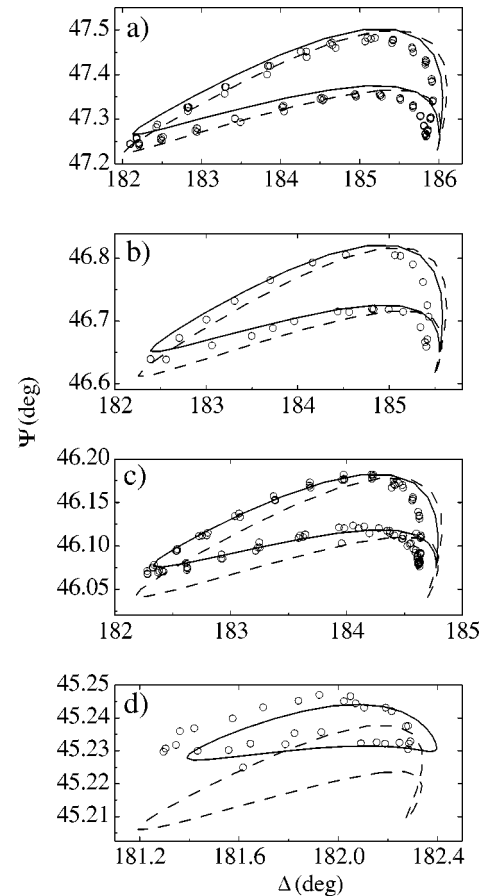


FIG. 9. (a), (b), (c), and (d) show data (circles) and simulations (lines) of the  $\Psi$  versus  $\Delta$  curves of (14PMB)Cl for  $N = 11, 9, 7$ , and  $3$  layers, respectively. The simulations shown with solid lines have a reduced surface tilt of  $27^\circ$  and a surface layer spacing of  $48.8 \text{ \AA}$ , except for (d) which uses a surface layer spacing of  $49.6 \text{ \AA}$ . All other optical parameters are from thick film simulations. The dashed lines are a simulation using the thick film results for the optical parameters.

formed a more thorough study of  $C_{8,12}$  as a function of thickness; 30 films up to  $N = 55$  layers have been studied whereas before we had only studied  $N \leq 20$  layers. From this study we found that the simulated  $\theta$  depends upon thickness. We found that  $N$  must be more than approximately 23 layers for our measurement of  $\theta$  to be representative of a bulk value. This is because our experimental technique is an integrating technique and so is primarily sensitive to the average value of  $\theta$ . Previously we did not realize this, so our fitting results for the optical parameters were not as precise as the fitting results presented here.

For reference the fitting results for thick films are given here. For  $C_{9,12}$  we found that  $\theta = 45.0 \pm 1^\circ$ ,  $\phi = 32.4 \pm 0.6^\circ$ ,  $n_e = 1.710 \pm 0.003$ , and  $n_o = 1.472 \pm 0.003$ . For  $C_{8,12}$  we obtained  $\theta = 45.0 \pm 1^\circ$ ,  $\phi = 32.0 \pm 1^\circ$ ,  $n_e = 1.703 \pm 0.003$ , and  $n_o = 1.468 \pm 0.003$ .

Because ellipsometry is an integrating technique and our simulation procedure assumes that all layers have the same tilt, the simulated value of  $\theta$  is representative of the value of  $\theta$  averaged over the film. We observed that the simulated

value of  $\theta$  decreases with film thickness. For (14PMB)Cl this procedure suggests that the surface layers are tilted at  $28 \pm 2^\circ$ . For  $C_{8,12}$  and  $C_{9,12}$  we found that the surfaces are tilted at  $40 \pm 2^\circ$ . These results are independent of the optical model used to describe the data.

Figure 9 shows the data for four thin films of (14PMB)Cl at  $120^\circ$ . The data are shown with circles. The solid line is the fit using a reduced surface tilt and increased surface layer spacing, while all other parameters are from the thick film fitting results. The dashed lines show the simulations using a uniform tilt and the optical parameters from thick films. The fit to the  $\Psi$  versus  $\Delta$  curve using a uniform tilt becomes better as the thickness increases suggesting that there is a surface effect. Specifically, two observations suggest the existence of a surface layers with reduced tilt. First, the simulations using a uniform tilt are offset from the data in  $\Psi$ , suggesting that the optical thickness is greater than this model predicts. This can be most clearly seen in Fig. 9(d). The optical thickness is greater if the surfaces have a reduced tilt because this leads to a greater layer spacing on the surface. Second, the width of the  $\Psi$  versus  $\Delta$  curve is too large in the uniform tilt model. A reduced surface tilt implies that the optical structure will be slightly less anisotropic, and thereby cause the width of the  $\Psi$  versus  $\Delta$  curve to decrease.

#### IV. DISCUSSIONS

To within our resolution,  $\theta$  is independent of temperature and  $d$  decreases with increasing temperature. This leaves a lingering question as to what is happening. Our simulations find that  $\phi$  increases with increasing temperature, which should cause the observed effect in  $d$ , although the angular change is too small by about a factor of 2 to cause the ob-

served change in  $d$ . There are two other likely explanations for these results. The conformation of the unusually long alkyl tails on these molecules may change with temperature. Alternatively, the interpenetration of adjacent layers may change with temperature.

We are surprised to find that the surface layers in the B2 phase are less tilted than the interior layers. For rod-shaped compounds it is found that the surface induces a greater tilt at the surface than found in the interior layers. This difference may be due to the fact the steric interactions play such an important role in the structure of the B2 phase. More detailed studies are required.

In conclusion, we have measured the optical tilt angle as a function of temperature in a compound possessing a 59 K wide B2 phase window. We have found that the tilt angle is independent of temperature over a 59 K temperature range to within our resolution of  $1^\circ$ . The data suggest that if  $\theta$  is a principal order parameter for the isotropic to B2 phase transition, then that phase transition is strongly discontinuous. Our results from one-layer films have allowed us to refine our optical model for the B2 phase. We have observed an unusual reduced tilt angle at the free surface of free-standing films in the B2 phase for three compounds. An enhanced surface tilt is usually seen at the surface of free-standing films using conventional rod-shaped molecules.

#### ACKNOWLEDGMENTS

We acknowledge L. Sauer for helping with the x-ray diffraction. The research was supported in part by the National Science Foundation, Solid State Chemistry Program under Grant Nos. DMR-9703898 and INT-9815859.

- 
- [1] R. B. Meyer, L. Liebert, L. Strzelecki, and P. Keller, *J. Phys. (France) Lett.* **36**, L69 (1975).
  - [2] A. D. L. Chandani, E. Gorecka, Y. Ouchi, H. Takezoe, and A. Fukuda, *Jpn. J. Appl. Phys., Part 2* **28**, L1265 (1989).
  - [3] J. Watanabe, Y. Nakata, and K. Shimizu, *J. Phys. II* **4**, 581 (1994).
  - [4] T. Niori, T. Sekine, J. Watanabe, T. Furukawa, and H. Takezoe, *J. Mater. Chem.* **6**, 1231 (1996).
  - [5] D. R. Link, G. Natale, R. Shao, J. E. MacLennan, N. A. Clark, E. Körblova, and D. M. Walba, *Science* **278**, 1924 (1997).
  - [6] D. A. Olson, M. Veum, A. Cady, M. V. D'Agostino, P. M. Johnson, H. T. Nguyen, L. C. Chien, and C. C. Huang, *Phys. Rev. E* **63**, 041702 (2001).
  - [7] W. Weissflog, L. Kovalenko, I. Wirth, S. Diele, G. Pelzl, H. Schmalfuss, and H. Kresse, *Liq. Cryst.* **27**, 677 (2000).
  - [8] A. Roy, N. V. Madhusudana, P. Tolédano, and A. M. F. Neto, *Phys. Rev. Lett.* **82**, 1466 (1999); P. Tolédano, O. G. Martins, and A. M. F. Neto, *Phys. Rev. E* **62**, 5143 (2000).
  - [9] S. Dumrongrattana, C. C. Huang, G. Nounesis, S. C. Lien, and J. M. Viner, *Phys. Rev. A* **34**, 5010 (1986).
  - [10] T. P. Reiker, N. A. Clark, G. S. Smith, D. S. Parmar, E. B. Sirota, and C. R. Safinya, *Phys. Rev. Lett.* **59**, 2658 (1987).
  - [11] W. Weissflog, Ch. Lischka, S. Diele, G. Pelzl, and I. Wirth, *Mol. Cryst. Liq. Cryst.* **328**, 101 (1999).
  - [12] R. M. A. Azzam and N. M. Bashara, *Ellipsometry and Polarized Light* (North-Holland, Amsterdam, 1989).
  - [13] D. A. Olson, A. Cady, P. M. Johnson, X. F. Han, and C. C. Huang (preprint).
  - [14] D. W. Berreman, *J. Opt. Soc. Am.* **62**, 502 (1972).
  - [15] E. B. Sirota, P. S. Pershan, L. B. Sorensen, and J. Collet, *Phys. Rev. A* **36**, 2890 (1987).